

Silicon avalanche photodiodes developed at the Institute of Electron Technology

Iwona Węgrzecka*, Maciej Węgrzecki, Jan Bar, Maria Grynglas, Andrzej Uszyński,
Remigiusz Grodecki, Piotr Grabiec, Sylwester Krzemiński, Tadeusz Budzyński,
Institute of Electron Technology, Al. Lotników 32/46, 02-668 Warsaw, Poland

ABSTRACT

Silicon avalanche photodiodes (APDs) - due to the effect of avalanche multiplication of carriers in their structure - are most sensitive and fastest detectors of visible and near infrared radiation. Also the value of noise equivalent power NEP of these detectors is the smallest. In the paper, the design, technology and properties of the silicon avalanche photodiodes with a $n^+ - p - \pi - p^+$ epiplanar structure developed at the Institute of Electron Technology (ITE) are presented. The diameters of photosensitive area range from 0.3 mm to 5mm. The ITE photodiodes are optimised for the detection of the 800 nm \div 850 nm radiation, but the detailed research on spectral dependencies of the gain and noise parameters has revealed that the spectral operating range of the ITE photodiodes is considerable wider and achieves 550 \div 1000 nm. These photodiodes can be used in detection of very weak and very fast optical signals. Presently in the world, the studies are carried out on applying the avalanche photodiodes in detection of X radiation and in the scintillation detection of nuclear radiation.

Keywords: Silicon avalanche photodiode, silicon photodiode, photodetector

1. INTRODUCTION

Silicon avalanche photodiodes (APDs) are very sensitive and high-speed detectors of visible and near infrared radiation ($\lambda < 1100\text{nm}$). Due to the phenomenon of the avalanche multiplication of carriers, APD are singled out by a very high current gain. Both, the outstanding signal gain and suitable noise properties of APDs cause that they achieve the highest signal-to-noise ratio, hence the lowest noise equivalent power (the highest detectivity) among all known so far detectors. Since the generation and transport of carriers in modern avalanche photodiode structures are very fast events and values of the RC factor are rather low, avalanche photodiodes are not only very sensitive but also very fast photodetectors.

Six types of silicon avalanche photodiodes were developed at the ITE. The diameters of photosensitive areas stretch from 0.3 to 5mm. These photodiodes are optimised for the detection of the radiation of $\lambda = 800 \div 850\text{ nm}$, however their performance spectral range is much wider and extends from 550 nm to 1100 nm.

The ITE APDs are characterised by excellent parameters and high reliability. The developed design and technology enabled their production at ITE with both high repeatability and yield. For developing and launching the production of these APDs- destined mainly for the American market - the ITE's research team was given numerous prestigious awards among which the most outstanding is the Economic Prize of the President of the Republic of Poland in the Category Invention of Product or Technology Development.

The avalanche photodiodes are indispensable for the detection of very weak and fast changing optical signals, they find application in many fields of science and technology, among the others in automation techniques, medicine, environment protection, geodesy, military techniques. Presently in the world, the studies are carried out on using the avalanche photodiodes in the detection of X radiation and the scintillation detection of nuclear radiation.

The principle of avalanche photodiode performance and the design, technology and properties of silicon avalanche photodiodes developed at the ITE are presented below

* e-mail: iwegrz@ite.waw.pl

2. PRINCIPLE OF AVALANCHE PHOTODIODE PERFORMANCE

The principle of APDs performance is based on the internal photoelectric phenomenon - generation and transportation of optically generated carriers in their structures - and on the effect of avalanche multiplication of carriers in the semiconductor p-n junction. The photoelectric phenomenon is characterised above all by the quantum efficiency and resulting from it the photoelectric sensitivity (called the primary sensitivity) which strongly depends on a wavelength (see chapter 4, Fig. 6.).

The APDs of modern design with an avalanche built-in region inside the PIN structure are characterised by the high primary sensitivity, high detection speed (as for the PIN photodiode) and high internal current gain (avalanche multiplication coefficient) - resulting from avalanche multiplication of carriers. Another important parameter of APDs is an avalanche noise, which comes from statistical fluctuation in the multiplication process. The avalanche (multiplication) noise determines about APDs noise properties and is characterised by an excess noise factor F .

The avalanche phenomenon can happen if the electric field in the p-n junction is higher than so called critical field (about 1×10^5 V/cm in Si), that is necessary for the impact ionisation to occur.

A chain of these ionisation impacts leads to carrier multiplication. The average number of electron - hole pairs created by one carrier per unit distance (of 1 cm) is named an impact ionisation coefficient. In case of silicon APDs, an electron ionisation coefficient (α) is considerable higher than a hole ionisation coefficient (β). The higher is electric field - the higher is ionisation coefficients of the holes and electrons, so the higher becomes the current gain. However, with the rise of the electric field the ratio of α/β becomes lower hence depending on it the excess noise factor F rises [1,2,3]. The maximum value of electric field in the avalanche region of Si APDs can extend from 2 to 5×10^5 V/cm. The choice of value of electric field in an APD structure constitutes the compromise between the demand for a high M and a reasonable low value of F factor. Most often, silicon APDs are designed in such way so the electric field at the junction plane of an avalanche region is not lower than 2×10^5 V/cm and not higher than 3.5×10^5 V/cm.

The gain and avalanche noise depend on the thickness of an avalanche region (the larger it is, the higher is gain but the lower F). They also depend on the participation of electron current in the total current injected into the avalanche region (the higher is an electron participation the highest is M and the lower is F). The thickness of build-in avalanche region is most often not smaller than $2 \mu\text{m}$ but doesn't exceed $10 \mu\text{m}$. The absorption region of high resistivity should be of the π type. Thus, from optically generated electron-hole pairs in the π region, only electrons are injected into the avalanche region. The schematic representation of electric field distribution in the structure of the silicon ITE APD is presented in Figure 1.

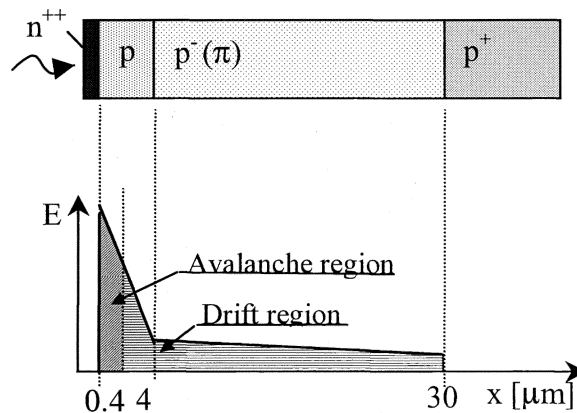


Fig. 1. Schematic profile of electric field for an ITE APD structure.

The structure is illuminated from the side of n^+ region. Absorption of photons and generation of electron-hole pairs, take place in an n^+ region for $\lambda < 400$ nm, in n^+ and p regions for $400 < \lambda < 500$ nm and in n^+ , p and π regions for $\lambda > 500$ nm. It results from the photon distribution in silicon for different wavelengths (see Figure 2).

If the n^+ and p regions are sufficiently narrow and the width of π region is appropriately wide, then at the infrared radiation of $\lambda > 800$ nm, most of carriers are generated in the π region.

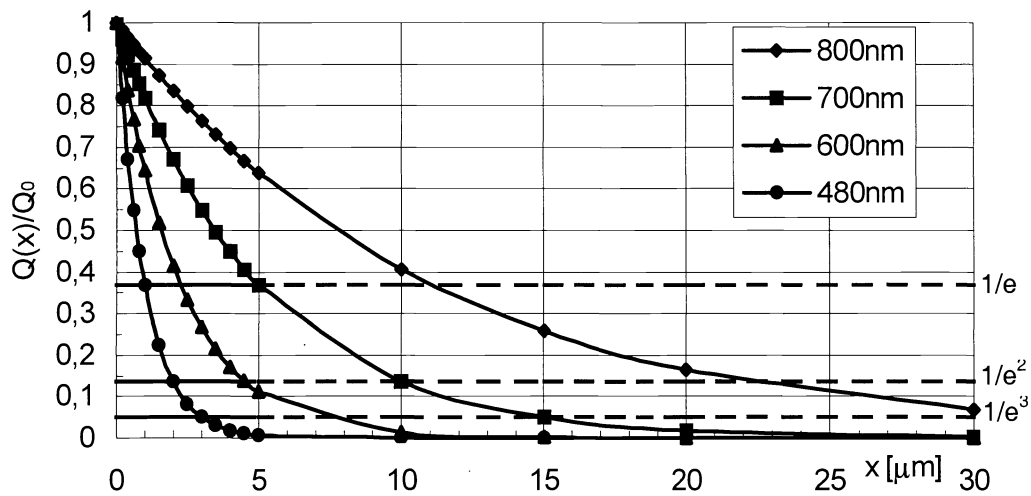


Fig. 2. Relative distribution of photons in silicon for different wavelengths of radiation

In Figure 3 the example of typical gain dependence on the reverse bias voltage for an APD (the ITE APD) is shown. As the voltage increases up to 50 V the p type avalanche region is being depleted from carriers. The increase of U_R over this value causes depletion of the π region. At about 100V, both avalanche and absorption regions are emptied from carriers. Further increase of bias voltage results in the rise of electric field in the structure. When it reaches the value higher then critical strength - multiplication of carriers occurs.

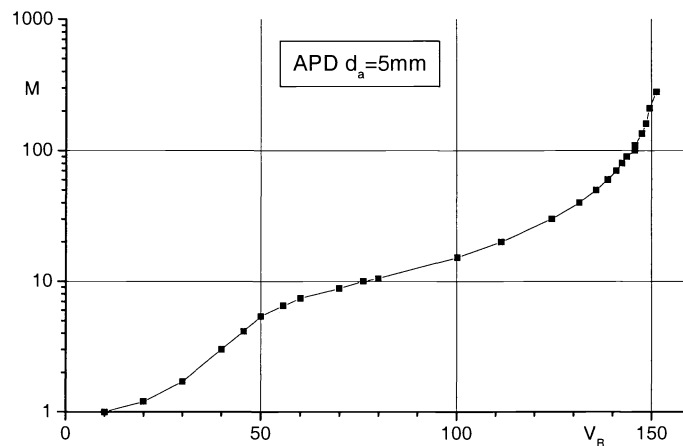


Fig. 3. Gain dependence on voltage of silicon APD

Further rise of reverse voltage causes that current density reaches the value for which the effect of avalanche breakdown takes place. This threshold voltage is named avalanche breakdown voltage.

3. DESIGN AND TECHNOLOGY OF SILICON AVALANCHE PHOTODIODES

Silicon APDs developed at ITE are characterised by an $n^+ - p - \pi - p^+$ structure with a hyper-abrupt $n^+ - p$ junction in centre of a photosensitive region, forming an avalanche region in the p type layer. The initial material is the 3" silicon wafer with the $30 \div 35 \mu\text{m}$ thick, high resistive ($\rho = 250 \div 300 \Omega\text{cm}$) epitaxial layer on the p^+ substrate of $\langle 111 \rangle$ crystallographic orientation.

The hyper-abrupt $n^+ - p$ junction (of $\sim 0.4 \mu\text{m}$ depth), is made by method of arsenic diffusion from amorphous silicon (doped during its deposition) to the p region (about $4 \mu\text{m}$ thick) that was previously obtained by implantation method and then by boron re-diffusion. The active region is surrounded by a n type sub-contact ring and a p^+ type stopper ring that stops space charge at the SiO_2/Si interface. The 140 nm thick, antireflective SiO_2 layer covers the active surface of the photodiode. Inactive regions are coated by silicon nitride layer and covered by aluminium.

The cross-section of an avalanche photodiode structure, optimised for $\lambda = 800 \div 850 \text{ nm}$ is shown in Figure 4.

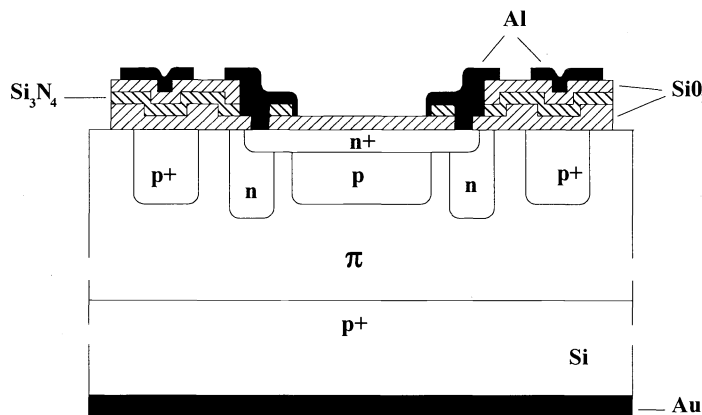


Fig. 4 Cross section of an ITE APD structure

The width of π region, ensures the high quantum efficiency of the inner photoelectric phenomenon therefore high primary sensitivity of the photodiode for this spectral range. The chosen thickness of n^+ , p and π regions ensure large participation of electrons in the avalanche phenomenon for radiation of $\lambda > 800 \text{ nm}$. The most difficult designing task is to calculate the optimal distribution of impurity concentration in the p type region, and subsequently to work out the key technological processes of forming the p and n^+ regions as well as optimal sequences of technological processes. The distribution of impurity concentration in the p type region should ensure required distribution of electric field in the avalanche region. Technological processes, especially thermal treatments should not degrade a junction of the avalanche region. Developing technology for APD structure required solving many problems connected with thermal treatment of wafers, accuracy and repeatability of parameters of technology processes and with widely called "cleanliness" of technological line.

"Quality" of the technological process is responsible for obtaining proper I-V characteristic, possible low dark current and conditioned on it low spectral density of dark noise current of APDs. The technological process of APD structures comprises about 30 partial processes, the most important are mentioned below.

The bulk design and technology of structure are common for all developed types of ITE APDs. The APD structures of different diameters of the active region are obtained by using different photo-masks in the procedure of APD processing.

In Figure 5 a wafer with the 5 mm APD structures are shown.

Avalanche photodiode structure - main technological processes

1. Thermal oxidation
2. 1st photolithography of SiO₂
3. Phosphorous pre-diffusion into an sub-contact region
4. Thermal oxidation
5. 2nd photolithography of SiO₂
6. Boron implantation into a channel stopper
7. Annealing
8. 3rd photolithography of SiO₂
9. Boron implantation into an active region
10. Boron re-diffusion
11. 4th photolithography of SiO₂
12. Arsenic diffusion
13. Si₃N₄ deposition
14. annealing of Si₃N₄
15. 5th photolithography so called yellow photo
16. Plasma etching of Si₃N₄
17. Chemical etching of SiO₂
18. SiO₂ deposition
19. Annealing of SiO₂
20. 6th photolithography of SiO₂
21. Al evaporation
22. 7th photolithography of Al
23. Al annealing
24. Treatment of a back-side
25. Au evaporation
26. Au annealing

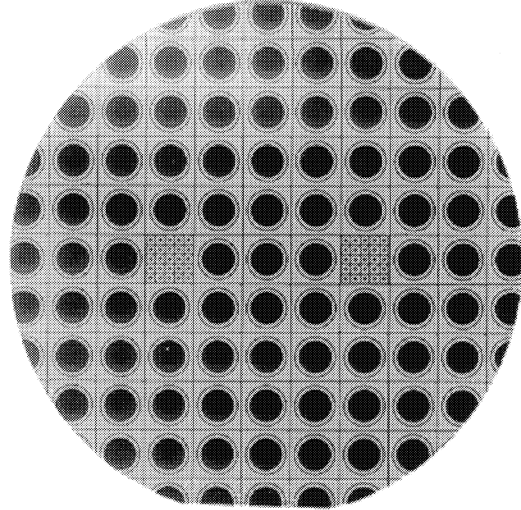


Fig. 5. The photograph of a wafer with APD structures of 5 mm active area diameter

4. SILICON AVALANCHE PHOTODIODES CHARACTERISTICS

Considerations concerning such avalanche photodiode parameters as the primary photoelectric sensitivity (at $M = 1$) and cut off frequency are similar to those as in case of PIN photodiodes. Whereas, the parameters that are conditioned by the avalanche multiplication effect, are determined by a gain (M), dark current (I_{R0}), noise current (I_N) and excess noise factor (F). For a given optical signal (first of all for $\lambda = \text{cons.}$) these parameters in essential way depend on a reverse bias voltage (V_R) and an operating temperature T (junction temperature).

Values of "avalanche" parameters of a photodiode at a given operating voltage (at fixed λ and T) determine about a signal to noise ratio, a noise equivalent power (NEP) and resulting from it detectivity D or D^* (detectivity normalised to the unit of detector area 1cm^2). In correctly processed photodiode structures, their noise is of shot nature. The dependencies of total noise and dark noise on gain are given in formulas (1) and (2). The formula (3) defines the excess noise factor, consecutive formulas (4) define the noise equivalent power and detectivity.

$$I_N = \{2q(I_{P0} + I_{B0})M^2 F(M) + I_{S0}\} \Delta f \quad (1)$$

$$I_N = \{2qI_{B0}M^2 F(M) + I_{S0}\} \Delta f \quad (2)$$

$$F(M) = I_{NP}^2 / 2qI_{P0}M^2 \Delta f \quad (3)$$

$$NEP = \frac{I_N / \Delta f^{1/2}}{S_{\lambda 0} \times M} \quad D = \frac{S_{\lambda 0} \times M}{I_N / \Delta f^{1/2}} \quad D^* = \frac{S_{\lambda 0} \times M \times A_d}{I_N / \Delta f^{1/2}} \quad (4)$$

I_{p0} – primary photoelectric current,
 I_{s0} – surface dark current,

I_{B0} – primary bulk dark current
 Δf – bandwidth, A_d – detector area in cm^2

Properties of the ITE APDs in the 800 ÷ 850 nm spectral range

At $\lambda = 800 \div 850$ nm, quantum efficiency of the ITE APDs exceeds the value of 70% and the primary sensitivity ($S_{\lambda 0}$) achieves the value of 0.5 A/W. The spectral characteristic of $S_{\lambda 0}$ for these APDs is presented in Fig 6. In Figures 7 and 8 there are examples of the $M(V_R)$, $I_{R0}(V_R)$ characteristics at different operating temperatures for the 3 mm photodiodes and in Figures 9 and 10 the dependencies of the noise current and NEP on gain M at different operating temperatures.

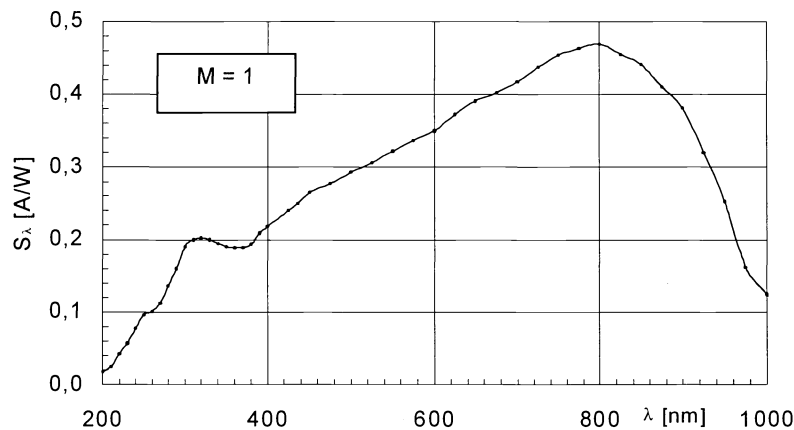


Fig. 6. Spectral characteristic of primary sensitivity of ITE APD.

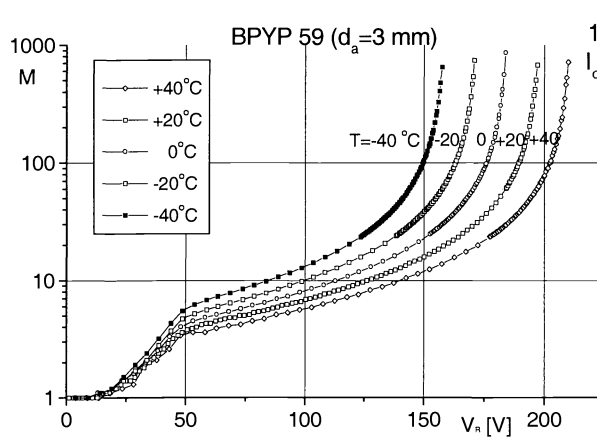


Fig. 7. Dependence of gain on reverse bias voltage at different temperatures for the 3 mm APD

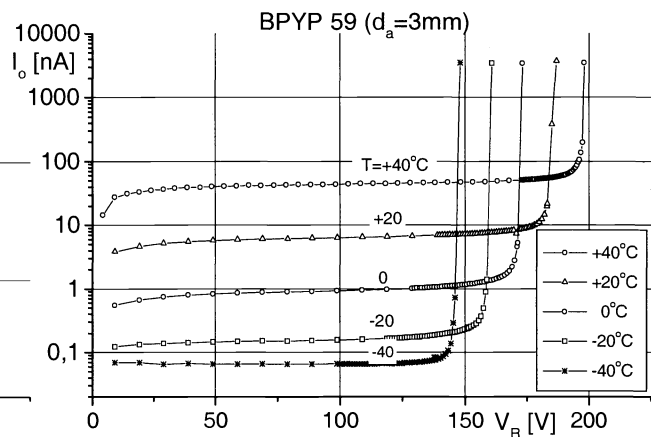


Fig. 8. Dependence of dark current on reverse bias voltage at different temperatures for the 3 mm APD

A gain at which the signal to noise ratio achieves a maximal value (NEP attains a minimal value) is called M_{opt} . Figures 11 and 12 illustrate the dependencies of NEP and detectivity D^* on the temperature. In Table 1, typical values of most important parameters at $\lambda = 830$ nm for 5 types APDs produced at the ITE are gathered.

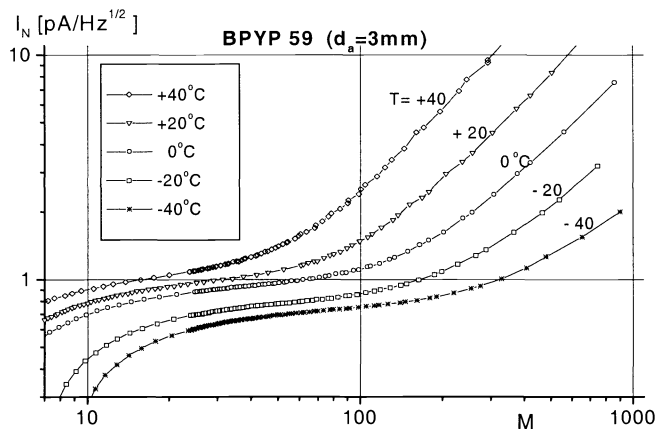


Fig. 9. Dependence of noise current on gain at different temperatures for the 3 mm APD

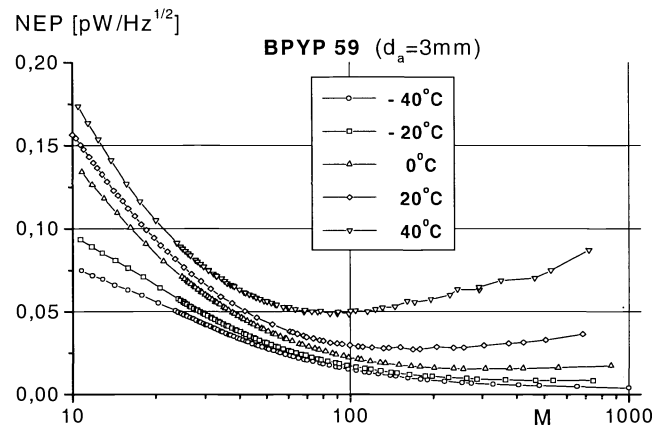


Fig. 10. Dependence of NEP on gain at different temperatures for the 3 mm APD

Table 1. Typical parameters of silicon avalanche photodiodes developed and produced at the ITE

Parameter	Symbol	Unit	BPYP 52 0.3 mm	BPYP 54 0.5 mm	BPYP 53 0.9 mm	BPYP 58 1.5 mm	BPYP 59 3 mm	Test conditions ¹⁾
Operating Voltage	V_R	V	180 ÷ 220 (min. 130 ÷ max. 280)					$M = 100$
Temperature Coefficient of V_R	α_{TR}	V/C	0.65					$M = 100$
$1/M \times dM/dT$		%/K	-3.3					$M = 50$
$1/M \times dM/dV$		%/V	6					$M = 50$
Sensitivity	S_λ	A/W	50					$M = 100$
Noise Current ²⁾	I_N	pA/Hz ^{1/2}	0.07	0.12	0.3	0.45	1	V_R at $M = 100$, $P_\lambda = 0$
Noise Equivalent Power	NEP	fW/Hz ^{1/2}	1.4	2.4	6	9	30	$M = 100$
Gain	M		800	600	480	240	100	$I_N = 1 \text{ pA/Hz}^{1/2}$
Sensitivity	S_λ	A/W	400	300	240	120	50	$I_N = 1 \text{ pA/Hz}^{1/2}$
Excess Noise Factor	$F(M)$		4					$M = 100$
Dark Current	I_0	nA	0.7	1.2	2.2	5	12	V_R at $M = 100$, $P_\lambda = 0$
Rise Time, Fall Time	t_r, t_f	ns	0.3	0.5	1	2	4.5	$R_L = 50 \Omega$, $M = 100$
Capacitance	C_{tot}	pF	1.7	3	7	12	40	V_R at $M = 100$, $P_\lambda = 0$
¹⁾ Test conditions $\lambda = 830 \text{ nm}$; $t_{amb} = 22 \text{ C}$ ²⁾ measured as the r.m.s. spectral density of dark noise current								

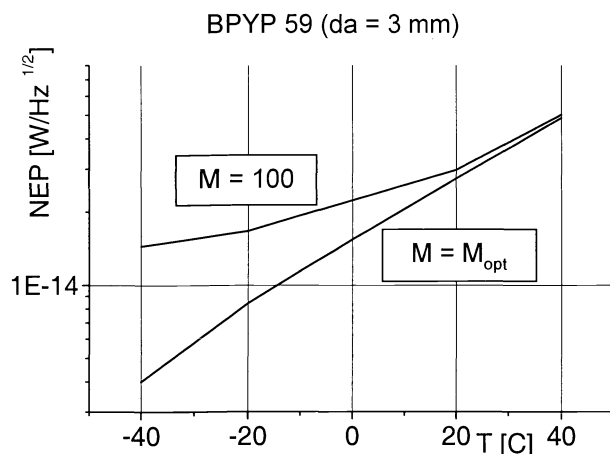


Fig. 11. Dependence of NEP on temperature at $M = 100$ and $M = M_{opt}$ for the 3 mm APD

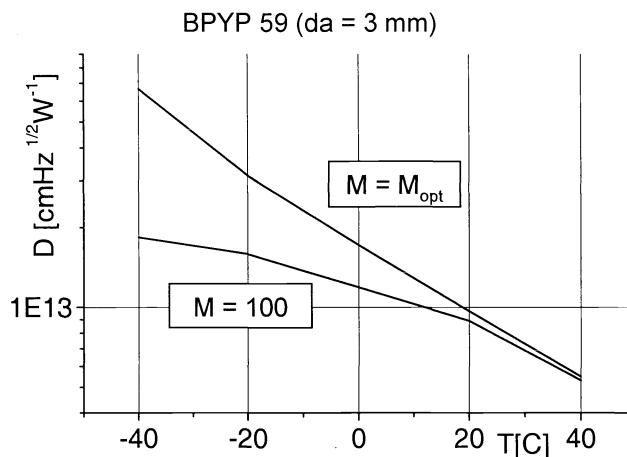


Fig. 12. Dependence of detectivity on temperature at $M = 100$ and $M = M_{opt}$ for the 3 mm APD

For example, for photodiodes with the photosensitive area of the 0.3 mm diameter a typical value of the noise current (I_N) at $M=100$ is below $0.1 \text{ pA/Hz}^{1/2}$ ($\text{NEP} = 1.4 \text{ fW/Hz}^{1/2}$), whereas for the photodiodes of the 3 mm diameter it is about $1 \text{ pA/Hz}^{1/2}$ ($\text{NEP} = 20 \text{ fW/Hz}^{1/2}$). The excess noise factor F amounts to value of 4 at $M = 100$ for all types of APDs. The temperature coefficient of operating voltage is 0.65 V/K . In Table 1 also “sensitivity” of gain to the changes in the bias voltage and operating temperature is presented. The ITE APDs are characterised by very high sensitivity and low noise, and those parameters are attained for relatively low operating voltages, typically 180-220 V (min 130 V, max 280 V); the breakdown voltages are about 10 V higher. High sensitivity and low noise of ITE APDs are due not only to their design, but also to technology that secures the high surface uniformity of the key parameters of an APD structure. This has been confirmed by the research on the uniformity of avalanche multiplication (gain) across the active surface of photodiodes that was carried out using the specially prepared for this purpose, the measurement setting. The example of the distribution of sensitivity at $M = 100$, for a photodiode of the 1.5 mm diameter is shown in Figure 13. The high surface uniformity enabled working out the APD with a photosensitive area of 5 mm diameter, which is a new development of the ITE. In Table 2 the basic parameters of the 5 mm APDs are presented.

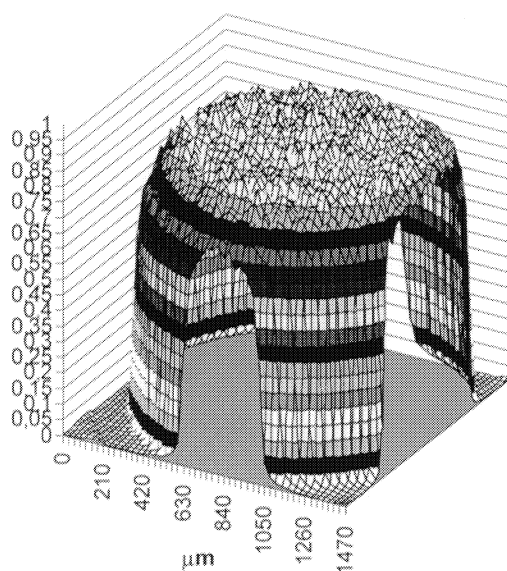


Fig. 13. Distribution of sensitivity on the surface of an 1.5 mm avalanche photodiode ($\lambda = 780 \text{ nm}$, spot $20 \text{ }\mu\text{m}$, modul $30 \text{ }\mu\text{m}$, $M = 100$, $P_i = 100 \text{ nW}$).

Table 2. Typical values of basic parameters of the 5 mm APD

Parameter	Symbol	Unit	Typical value	Test conditions ¹⁾
Operating Voltage	V_{R2}	V	180 ÷ 220	$I_N = 2 \text{ pA/Hz}^{1/2}$
Gain	M		160	V_R at $I_N = 1 \text{ pA/Hz}^{1/2}$
Dark Current	I_0	nA	90	V_R at $I_N = 1 \text{ pA/Hz}^{1/2}$
Sensitivity	S_λ	A/W	80	V_R at $I_N = 1 \text{ pA/Hz}^{1/2}$
Noise Equivalent Power	NEP	fW/Hz ^{1/2}	25	V_R at $I_N = 1 \text{ pA/Hz}^{1/2}$
Capacitance C_{tot}	C_{tot}	pF	110	$V_R = 100\text{V}$, $P_\lambda = 0$
Rise Time, Fall Time	t_r , t_f	ns	12	$R_L = 50\Omega$, $M = 100$
Test conditions: $\lambda = 830 \text{ nm}$; $t_{\text{amb}} = 20 \text{ C}$				

Properties of the ITE APDs in the 400-1000 nm spectral range.

The demand for scintillation detectors of nuclear radiation, in which a photodiode responds to very weak radiation emitted by scintillation material stimulated by nuclear radiation, has caused the increase of studies on silicon APDs for scintillation detection. Since the emission spectrum of known scintillating materials covers the 400 ÷ 650 nm range, hence the necessity of research on already developed ITE APDs at the short-wavelengths range arose. The studies on properties of APDs in their full operating spectral range, with special consideration of the short-wavelengths range were carried out. The APDs with larger diameters (1.5 mm, 3 mm, 5mm) were chosen because scintillation techniques require photodiode of possible largest photosensitive areas. The spectral dependencies of dark noise current (I_N) at the operating voltage, for which $M = 100$ and the spectral dependencies of gain (M) at the operating voltage, for which the dark noise current of a photodiode attains value of $2 \text{ pA/Hz}^{1/2}$ are shown in Figure 14. In Figure 15, the exemplary dependence of F on λ at different gains for the 5 mm photodiode is presented.

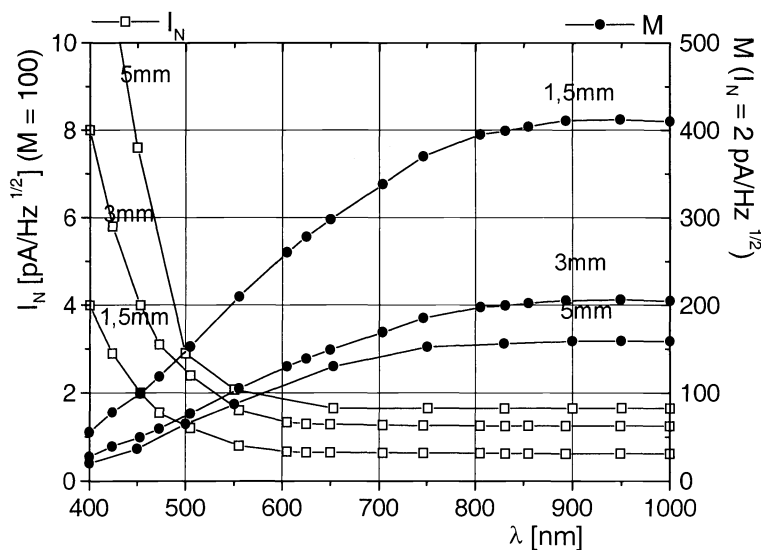


Fig. 14. Spectral dependencies of noise current and gain for the 1.5 mm, 3 mm and 5 mm APDs

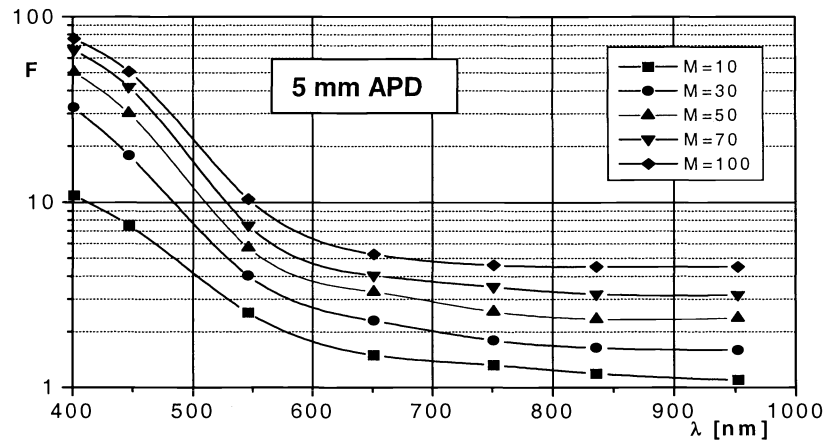


Fig. 15. Spectral dependencies of excess noise factor at different gains for the 5 mm APD

As it can be seen from above dependencies, the shorter is the wavelength of incident radiation the higher is noise current (I_N) and excess noise factor (F) at $M = \text{cons.}$, and lower is the gain (M) for $I_N = \text{cons.}$. Worsening of photodiode properties for shorter wavelengths results from the increase of number of holes participating in total current flowing through the avalanche region (see chapter 2). The spectral characteristics of total sensitivity S_λ ($S_\lambda = S_{\lambda 0} \times M$) at $I_N = 2 \text{ pA/Hz}^{1/2}$ are shown in Figure 16.

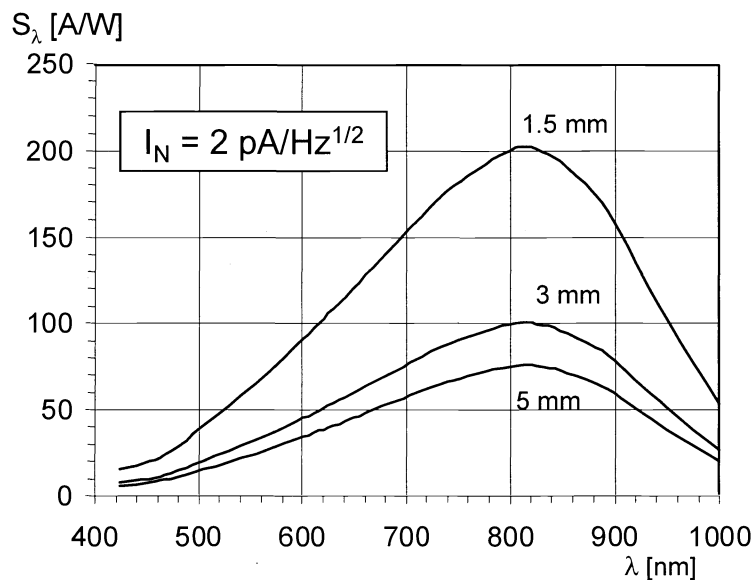


Fig. 16. Spectral characteristics of total sensitivity for the 1.5 mm, 3 mm and 5 mm APDs.

It can be concluded, from these dependencies, that the spectral operating range for the ITE APDs extends from 550 nm to 1000 nm.

In Figure 17 there are the photographs of the 3 mm and 5 mm photodiodes in metallic cases with flat glass windows. The examples of new applications of APDs are illustrated in Figures 18 and 19. The developed at the ITE module with an avalanche photodiode and a micro-cooler with a Peltier element is shown in Figure 18. Using the micro-cooler

ensures that photodiode operates at a constant temperature and improves photodiode parameters by lowering the operating temperature – in case of the two-steps micro-cooler up to $-40\text{ }^{\circ}\text{C}$.

In Figure 19 the scintillation fiber-optic detector developed at the ITE is presented. It comprises of an avalanche photodiode of the 1.5 mm diameter coupled with a scintillation optical fiber. These kind of scintillation detectors are now used for creating fiber optic arrays in which particles don't fall directly on detector. The scintillation detection of nuclear radiation, as well as possibilities of using avalanche photodiodes in these fields have resulted in the renaissance of interest in avalanche photodiodes.

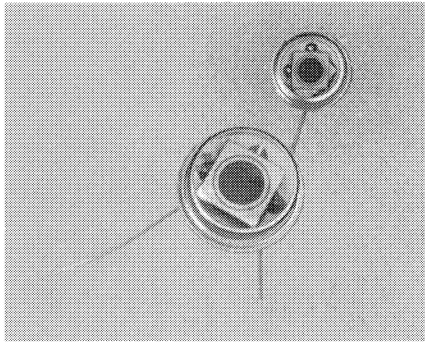


Fig. 17. Photograph of 3 mm and 5 mm APDs.

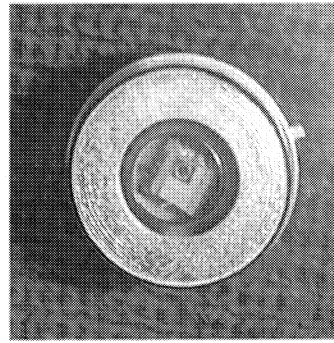


Fig. 18. Photograph of the module with an APD on micro-cooler.

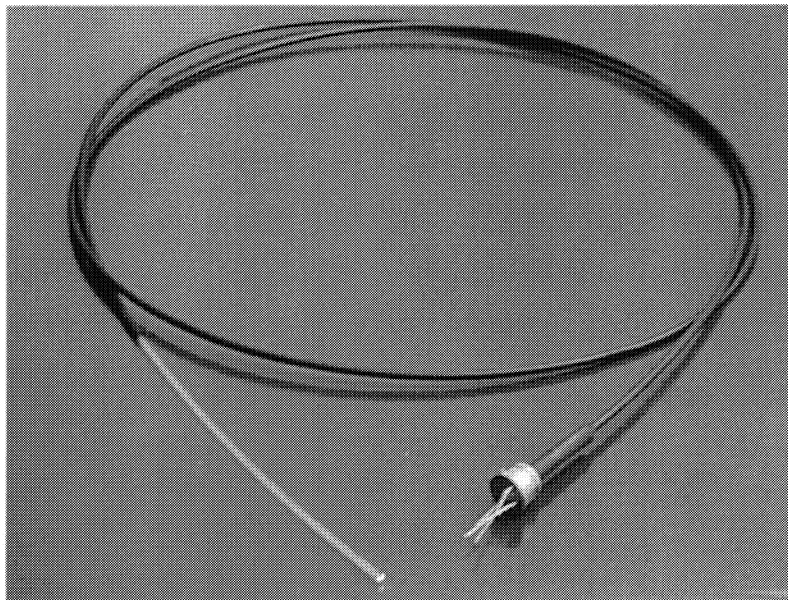


Fig. 19. Photograph of the scintillation fiber-optic detector with an 1.5 mm APD.

REFERENCES

1. G.E.Stillman, C.M Wolfe., *Avalanche Photodiodes*, Semiconductors and Semimetals, vol. 12 Infrared Detectors II, Academic Press, New York, 1977, 291-393
2. F.Capasso, *Physics of Avalanche Photodiodes*, Semiconductors and Semimetals, vol. 22 part D, AT&T Bell Laboratories, Academic Press, New York, 1985, 2-173
3. T. Kaneda, *Silicon and Germanium Avalanche Photodiodes*, Semiconductors and Semimetals, vol. 22 part D, AT&T Bell Laboratories, Academic Press, New York, 1985, 247-328
4. I. Węgrzecka, M. Węgrzecki, *The Properties of ITEE's Silicon Avalanche Photodiodes within the Spectral Range Used in Scintillation Detection*, Nucl. Instr. & Met. in Phys. Res. A, 426 (1999) 212-215
5. I. Węgrzecka, M. Grynglas, M. Węgrzecki, J. Bar, R. Grodecki, *Temperature characteristics of silicon avalanche photodiodes*, Proc. of SPIE Vol.4516, 194-201
6. I. Węgrzecka, M. Grynglas, M. Węgrzecki, *Spectral dependence of the main parameters of silicon avalanche photodiodes*, Proc. of SPIE Vol.4516, 187-193
7. J. Bar, E. Dobosz, I. Węgrzecka, M. Węgrzecki, *Design and technology of a scintillating fibre sensor with silicon avalanche photodiode*, Proc. of SPIE Vol.4516, 214-217
8. M. Moszynski, M. Kapusta, M. Balcerzyk, M. Szawlowski, D. Wolski, I. Węgrzecka, M. Węgrzecki, *Comparative study of avalanche photodiodes with different structures in scintillation detection*. IEEE Transactions on Nuclear Science, vol.48, no.4, pt.1, Aug. 2001., 1205-1210.